Role of Cholesterol in the Formation and Nature of Lipid Rafts in Planar and Spherical Model Membranes

Jonathan M. Crane and Lukas K. Tamm
Department of Molecular Physiology and Biological Physics and Biophysics Program, University of Virginia, Charlottesville, Virginia

ABSTRACT Sterols play a crucial regulatory and structural role in the lateral organization of eukaryotic cell membranes. Cholesterol has been connected to the possible formation of ordered lipid domains (rafts) in mammalian cell membranes. Lipid rafts are composed of lipids in the liquid-ordered (l_o) phase and are surrounded with lipids in the liquid-disordered (l_d) phase. Cholesterol and sphingomyelin are thought to be the principal components of lipid rafts in cell and model membranes. We have used fluorescence microscopy and fluorescence recovery after photobleaching in planar supported lipid bilayers composed of porcine brain phosphatidylcholine (bPC), porcine brain sphingomyelin (bSM), and cholesterol to map the composition-dependence of l_d/l_o phase coexistence. Cholesterol decreases the fluidity of bPC bilayers, but disrupts the highly ordered gel phase of bSM, leading to a more fluid membrane. When mixed with bPC/bSM (1:1) or bPC/bSM (2:1), cholesterol induces the formation of l_o phase domains. The fraction of the membrane in the l_o phase was found to be directly proportional to the cholesterol concentration in both phospholipid mixtures, which implies that a significant fraction of bPC cosegregates into l_o phase domains. Images reveal a percolation threshold, i.e., the point where rafts become connected and fluid domains disconnected, when 45–50% of the total membrane is converted to the l_o phase. This happens between 20 and 25 mol % cholesterol in 1:1 bPC/bSM bilayers and between 25 and 30 mol % cholesterol in 2:1 bPC/bSM bilayers at room temperature, and at ~35 mol % cholesterol in 1:1 bPC/bSM bilayers at 37°C. Area fractions of l_o phase lipids obtained in multilamellar liposomes by a fluorescence resonance energy transfer method confirm and support the results obtained in planar lipid bilayers.

INTRODUCTION

Since the discovery that mammalian cell membranes could be separated into fractions by cold extraction with nonionic detergents such as Triton X-100 (Mescher and Apgar, 1985; Brown and Rose, 1992), extensive studies have been conducted by cell biologists and biophysicists to discover the physical origin and to ascertain the biological significance of this phenomenon. A significant amount of data has been accumulated indicating that the insolubility of lipids in cold Triton X-100 correlates with the cholesterol concentration in cell and model membranes. This data has often been interpreted as evidence for the lipid bilayer phase in which the extracted lipids reside at the time of exposure, and it has been inferred that cell membranes contain coexisting phases of distinct lipid composition and viscosity (Ribeiro and Dennis, 1973; Simons and van Meer, 1988; Schroeder et al., 1994; Baird et al., 1999; London and Brown, 2000). In the absence of sterols, phospholipid bilayers exist in either a highly ordered gel phase or a liquid-disordered (l_d) phase, depending on whether the temperature is below or above the chain melting phase transition (T_m) for that lipid. Mixed model membranes containing high- and low-T_m phospholipids can contain coexisting gel and liquid-disordered (l_d) phases, but an intermediate phase, called liquid-ordered (l_o) that forms in the presence of cholesterol (Sankaram and Thompson, 1990), has been postulated to be the source of detergent resistance in cells (see Brown and London, 2000; Anderson and Jacobson, 2002; Edidin, 2003; for recent reviews). Liquid-ordered lipid domains, or rafts, are often thought to be responsible for the molecular sorting of membrane proteins into distinct regions of the cell membrane. Most evidence for this conjecture is indirect and centers on the finding that doubly acylated proteins, glycophosphatidylinositol (GPI)-anchored proteins, and some integral membrane proteins partition together with cholesterol and sphingomyelin into the insoluble fraction of cold Triton X-100 extracted cell membranes.

Cholesterol is the single most abundant lipid species in mammalian cell membranes. Ninety-percent of all cellular cholesterol resides in the plasma membrane, where it composes between 25 and 50% of the lipid, depending on the cell type (Bloch, 1991). Cholesterol is probably the most important lipid when it comes to controlling the size and area fraction of l_o phase domains in membranes. For rafts to have a strong effect on protein-protein or protein-lipid interactions in the membrane, and for the cell to have strict control over reaction rates between membrane-bound proteins, the fraction of the membrane in the l_o phase should be near a percolation threshold, where minute changes in lipid composition can result in global changes of the topology of membranes (Thompson et al., 1995). This is one possible reason for the elaborate system cells have evolved to maintain cholesterol homeostasis (Simons and Ikonen, 2000). Cholesterol is synthesized in the endoplasmic reticulum. It then travels to the Golgi where it combines with sphingolipids and from there it is believed to be transported to the plasma membrane in the form of rafts (Simons and Ikonen, 1997) or cholesterol-phospholipid complexes (McConnell and Vrljic,

Submitted October 10, 2003, and accepted for publication January 19, 2004.
Address reprint requests to Lukas K. Tamm, Tel.: 434-982-3578; Fax: 434-982-1616; E-mail: lkt2e@virginia.edu.

0006-3495/04/05/2965/15 $2.00

2003). Cholesterol can also be acquired from circulating lipoproteins through passive or receptor-mediated interactions. Likewise, these same lipoproteins continuously remove cholesterol from the plasma membrane to control its levels.

Binary mixtures of high-T_m phosphatidylcholines (PC) and cholesterol, as well as ternary mixtures of low-T_m PCs, cholesterol, and high-T_m PCs or sphingomyelin (SM), exhibit coexisting l_d and l_o phases (Recktenwald and McConnell, 1981; Sankaram and Thompson, 1990; Silvius et al., 1996; Feigenson and Buboltz, 2001). The l_o phase lipid domains can be visualized by fluorescence microscopy in giant vesicles composed of SM, fluid PCs, and cholesterol (Dietrich et al., 2001a; Veatch and Keller, 2002; Kahya et al., 2003; Baumgart et al., 2003). They may also be observed by epifluorescence microscopy in planar supported lipid monolayers (Dietrich et al., 2001a,b; Kahn et al., 2003), in planar supported lipid bilayers (Dietrich et al., 2001a), in unsupported planar lipid bilayers (Samsonov et al., 2001), or by atomic force microscopy in planar supported lipid bilayers (Rinia et al., 2001; Saslowsky et al., 2002; Yuan et al., 2002).

Supported lipid bilayers provide a convenient and unique way to study lipid rafts. They can be made relatively quickly, with strict control over the lipid composition. A water-filled cleft of ~2 nm exists between the solid support and lipid bilayer (Kiessling and Tamm, 2003) and preserves the fluidity and thermal phase transitions of supported bilayers (Tamm and McConnell, 1985; Tamm, 1988). In addition to direct observation by epifluorescence microcopy, the lateral mobility of appropriate fluorescent probes can be measured by fluorescence recovery after photobleaching or single molecule tracking, and the binding kinetics of fluorescent ligands on and off the surface may be studied by total internal reflection fluorescence microscopy. Although some questions remain about the influence of the solid support on some aspects of supported bilayers, the planar geometry greatly facilitates the interpretation of structural and dynamic data obtained in this system. Most previous fluorescence studies on rafts in supported membranes have used supported monolayers on microscope slides that were derivatized with long alkyl chains (Dietrich et al., 2001a,b; Kahn et al., 2003). In seeking to use supported lipid bilayers for studies of lipid rafts, we examine in this work the role that cholesterol plays in the formation, nature, and possible function of coexisting lipid phases on solid supports. We also examine the suitability of various lipid probes for imaging rafts by epifluorescence microscopy and measuring their mobilities in raft lipid mixtures by fluorescence recovery after photobleaching (FRAP). Finally we correlate raft area fractions obtained in supported bilayers by epifluorescence microscopy with area fractions obtained in multilamellar liposomes of identical composition by fluorescence resonance energy transfer (FRET).

MATERIALS AND METHODS

The following materials were purchased and used without further purification: POPC, porcine bPC, porcine bSM, NBD-DPPE, NBD-DOPE, Rh-DOPE, and Rh-DPPE from Avanti Polar Lipids (Alabaster, AL); $DiIC_{12}$ and $DiIC_{18}$ from Molecular Probes (Eugene, OR); cholesterol, *n*-octyl β-D-glucopyranoside (β-OG), and HEPES from Sigma Chemical (St. Louis, MO); chloroform, ethanol, methanol, NaCl, NaOH, Contrad detergent, sulfuric acid, and hydrogen peroxide from Fischer Scientific (Fair Lawn, NJ). Water was purified first with organic, free, and deionizing filters (Virginia Water Systems, Richmond, VA), and then in a NANOpure system (Barnstead International, Dubuque, IA) to reach a resistivity of 18.2 MΩ/cm.

Planar bilayers were prepared on quartz slides (Quartz Scientific, Fairport Harbor, OH) by the Langmuir-Blodgett/Schäfer method (Tamm and McConnell, 1985; Tamm and Tatulian, 1997). Slides were cleaned by boiling in 1% Contrad detergent, followed by sonication for 30 min before extensive rinsing with water. Residual organic material was removed by immersion in a ''piranha'' solution of three parts sulfuric acid to one part 30% hydrogen peroxide (v/v) for 10 min, followed by extensive rinsing in water. Immediately before use, the slides were further cleaned in an argon ion plasma sterilizer (Harrick Scientific, Ossining, NY). All monolayers were prepared on a subphase of pure water in a Langmuir-Blodgett trough system with computer feedback to control surface pressure, compression speed, and dipping of the substrate (Nima Technology, Coventry, England). Films were first compressed from zero surface pressure to 35 mN/m, then expanded back to 32 mN/m and allowed to equilibrate for at least 10 min at this pressure before deposition onto the slide. Surface area was monitored during dipping to record the transfer ratio, which was always between 90 and 110% of the slide area. After touchdown to complete the bilayer, planar membranes were soaked in HEPES buffer (10 mM HEPES, 150 mM NaCl, pH 7) for 30 min.

Imaging and lateral diffusion studies were performed with a laser and fluorescence microscopy system that has been described in detail previously (Tamm, 1988; Kalb et al., 1992; Wagner and Tamm, 2000). Images were recorded by a Cooke Sensicam QE charge-coupled device camera cooled to −12°C (Cooke, Auburn Hills, MI). Image analysis and data acquisition from FRAP was done using LabVIEW software (National Instruments, Austin, TX). FRAP was performed by bleaching the membrane in a pattern of parallel stripes (Smith and McConnell, 1978), and the data were fit to the model

$$F(t) = F_\infty + (F_0 - F_\infty)\exp(-Da^2t), \quad (1)$$

where F_0 and F_∞ are the initial and final fluorescence intensities after bleaching, respectively; $a = 2\pi/p$, p is the stripe period; and D is the lateral

TABLE 1

Abbreviations not defined in text	
$DiIC_{12}$	1,1′-Didodecyl-3,3,3′,3′-tetramethylindocarbocyanine perchlorate
$DiIC_{18}$	1,1′-Dioctadecyl-3,3,3′,3′- tetramethylindocarbocyanine perchlorate
DPPC	1,2-Dipalmitoyl phosphatidylcholine
HEPES	*n*-[Hydroxyethyl]piperizine-*n*′-[2-ethanesulfonic acid]
NBD-DOPE	1,2-Dioleoyl phosphatidylethanolamine-*n*-[7-nitro-2-1,3-benzoxadiazol-4-yl]
NBD-DPPE	1,2-Dipalmitoyl phosphatidylethanolamine-*n*-[7-nitro-2-1,3-benzoxadiazol-4-yl]
POPC	1-Palmitoyl-2-oleoyl phosphatidylcholine
Rh-DOPE	1,2-Dioleoyl phosphatidylethanolamine-*n*-[lissamine rhodamine B]
Rh-DPPE	1,2-Dipalmitoyl phosphatidylethanolamine-*n*-[lissamine rhodamine B]

diffusion coefficient. Stripes of 12.7, 7.9, and 3.2 μm periodicity, respectively, were used for membranes of decreasing fluidity. For membranes of intermediate fluidity, experiments with two different stripe periods were conducted and averaged. The percentage of fluorescence recovery was determined by

$$recovery = \frac{F - F_0}{F_{\text{pre}} - F_0} \times 200, \tag{2}$$

where F_{pre} is the fluorescence intensity before photobleaching. The fast fluorescence recovery fraction for an experiment, as shown in Fig. 2 *C* and Fig. 4 *A*, is the horizontal asymptote of a single exponential fit to the recovery curve (Fig. 2, *A* and *B*). All images and FRAP experiments were reproduced on different areas of multiple samples. The general appearances of the images and especially the measured area fractions were well reproducible although there are variations in size and shape of domains produced under identical conditions. A comparison of domains formed in the presence of different dyes, but with otherwise identical lipid compositions, gives some indication of this variability (Fig. 3).

Multilamellar liposomes were made by the following procedure: The appropriate lipids were mixed in chloroform or chloroform/methanol. The solvent was evaporated under a stream of nitrogen gas, then desiccated under vacuum for at least 1 h. The residue was resuspended in HEPES buffer, vortexed, and freeze-thawed five times by repeated immersion in liquid nitrogen followed by water at 40°C. Samples were then diluted to the desired concentration in HEPES buffer and stored overnight at 4°C. The overall concentration of fluorescently labeled lipids was kept at 1 μM, and the bulk lipid concentration was adjusted to get the desired dye/lipid ratio.

Fluorescence emission spectra were recorded with a Fluorolog-3 spectrofluorometer (Jobin-Yvon, Lille, France) with an excitation wavelength of 466 nm. Slits of the excitation double monochromator and the emission single monochromator were both set to 5 nm. Emission spectra were corrected for light scattering by subtracting background spectra of liposomes at the appropriate concentrations in the absence of fluorescent dye. Absorbance spectra were recorded with a Hitachi U-2000 UV/Vis spectrophotometer (Hitachi Instruments, Dublin, PA).

The efficiency of energy transfer between donor and acceptor molecules has a well-known dependence on the inverse sixth power of the distance r between the pair (Stryer, 1978),

$$E(r) = \frac{r^{-6}}{r^{-6} + R_0^{-6}}, \tag{3}$$

where R_0 is known as the Förster radius and is defined as the distance at which $E = 0.5$. From the emission spectrum of the donor and the absorbance spectrum of the acceptor, R_0 can be calculated as

$$R_0 = 9790(J\kappa^2 Q_0 n^{-4})^{1/6}, \tag{4}$$

where κ^2 is the orientation factor for the dipole-dipole interaction, Q_0 is the quantum yield of the donor, n is the refractive index of the medium, and J is the normalized spectral overlap integral,

$$J = \frac{\int F(\lambda)\varepsilon(\lambda)\lambda^4 d\lambda}{\int F(\lambda) d\lambda}, \tag{5}$$

and where $F(\lambda)$ is the emission intensity of the donor and $\varepsilon(\lambda)$ is the extinction coefficient of the acceptor at wavelength λ. In our calculations of R_0, we assume that $\varepsilon^2 = 2/3$ for random orientation (Stryer, 1978), $Q_0 = 0.75 \pm 0.15$ for NBD in a membrane (Connor and Schroit, 1987), and $n = 1.415 \pm 0.085$, which is the mean $\pm$ SD of n in water (Weast, 1983) and n in the hydrocarbon region of a bilayer (Connor and Schroit, 1987). Steady-state FRET is calculated as

$$E = 1 - F/F_0, \tag{6}$$

where F and F_0 are the donor emissions in the presence and absence of the acceptor, respectively. Emission intensities measured at 532 nm were used to determine E. Measured intensities were normalized for changes in dye concentration by dividing by the emission intensity at 532 nm after dissolving the liposomes in 50 mM β-OG, which relieved all FRET.

RESULTS

To better understand the role of cholesterol in the formation of domains in complex lipid mixtures, we first determined its effect on the individual raft component lipid species. Therefore, we mixed cholesterol with pure PC or SM and examined the morphology of the resulting bilayers by epifluorescence microscopy and their dynamic properties by FRAP. As expected, we found that cholesterol has divergent effects on the behavior of bilayers composed of PCs or SM (Figs. 1 and 2). When cholesterol is combined with POPC, no phase separation is visible up to the highest investigated mol fraction (50% mol/mol, Fig. 1 *A*), and the fast fluorescence recovery fraction remains consistently high in lateral diffusion experiments with NBD-DOPE as a fluorescent phospholipid tracer (Fig. 2 *C*). However, the lateral diffusion coefficient decreases monotonically from $\sim$1 μm^2/s in the absence of cholesterol to $\sim$0.3 μm^2/s at 50% cholesterol (Fig. 2 *D*). Cholesterol clearly reduces the fluidity and hence increases the viscosity of POPC bilayers. The behavior of PC from porcine brain extracts (bPC) is very similar to that of synthetic POPC up to 40% cholesterol (Fig. 1 *B* and Fig. *2*, C and *D*). However, at a cholesterol concentration of 50%, the majority of the bilayer excludes the Rh-DOPE dye, which becomes concentrated in numerous small inclusion domains that comprise 18 $\pm$ 2% of the total bilayer area (Fig. 1 *B*). Concomitant with this morphology change, the fast fluorescence recovery fraction of NBD-DOPE decreases to 60% at 50% cholesterol (Fig. 2 *C*). Therefore, bPC is less fluid than POPC at very high cholesterol concentrations. We do not know the composition and physical properties of the dye-including or dye-excluding domains in this case, but suspect that they are a result of the heterogeneity of the natural bPC mixture that was used in these experiments. According to the manufacturer, bPC contains $\sim$13% highly unsaturated and other unusual acyl chains. It is possible that PCs with these chains have a lower affinity for cholesterol and therefore phase-separate from bilayer areas that are rich in cholesterol and poor in Rh-DOPE.

Although cholesterol reduces the lipid mobility in PC bilayers, it has the opposite effect on bilayers of brain sphingomyelin (bSM). In the absence of cholesterol, bSM bilayers exhibit large star-shaped Rh-DPPE-excluding domains (Fig. 1 *C*). These dye-excluding domains probably

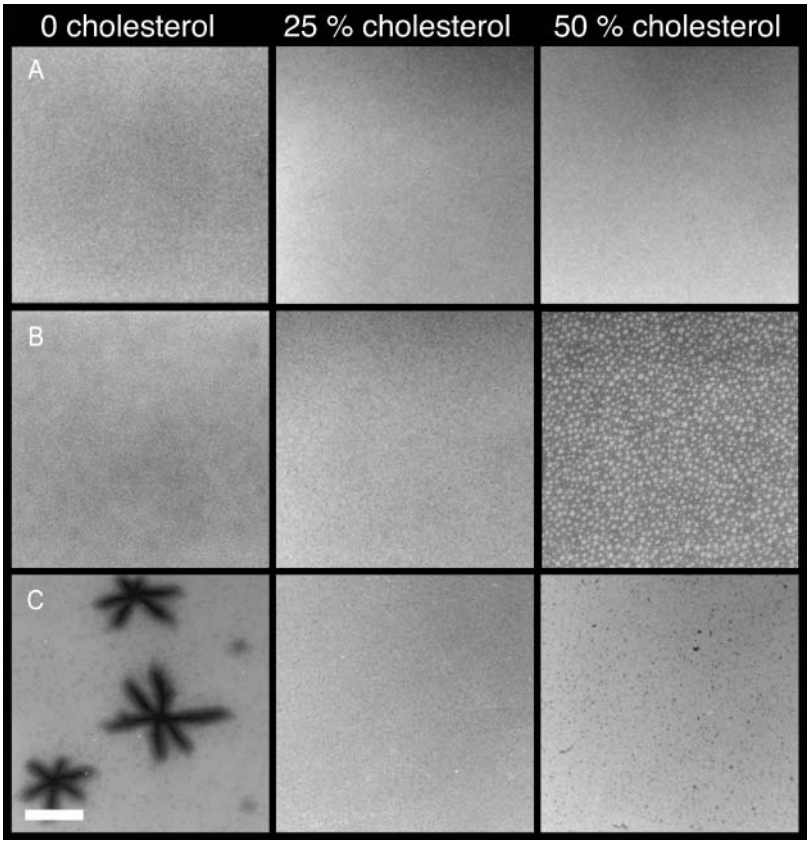

FIGURE 1 Fluorescence micrographs of bilayers of binary mixtures containing (*A*) POPC, (*B*) bPC, or (*C*) bSM, and cholesterol. Bilayers were formed by the Langmuir-Blodgett/Schäfer method on quartz slides. POPC and bPC bilayers were stained with 0.5% Rh-DOPE in the monolayer applied distally to the quartz support. The bSM bilayers were stained with 0.5% Rh-DPPE in the monolayer applied distally to the quartz support. Experiments were performed at room temperature. The white bar represents 20 μm.

reflect a segregation of the most rigid components in the heterogeneous mixture of natural bSM. Compared to the PC bilayers, almost no lateral diffusion is observed on the $\mu m^2/s$ length- and timescales (Fig. 2 *A*). The fast fluorescence recovery fraction of NBD-DPPE is $<20\%$ and its diffusion coefficient is <0.1 $\mu m^2/s$. The corrugated shapes of the stain-excluding domains and the lateral diffusion data indicate that the dark and bright areas of these bilayers are in a solid gel phase. (The bright areas may consist of submicroscopic dye-excluding domains and trapped NBD-DPPE-rich areas in between them—Hwang et al., 1995—that cannot be resolved by conventional epifluorescence microscopy.) The addition of cholesterol to bSM bilayers results in a disappearance of the dark domains (Fig. 1 *C*), and increases the fast fluorescence recovery fraction of NBD-DPPE to nearly 60% and lateral diffusion coefficient to ~ 0.2 $\mu m^2/s$ (Fig. 2, *B–D*) at 50% cholesterol. Therefore, the fluidities of bPC and bSM membranes are almost the same at equimolar cholesterol.

In the absence of cholesterol, mixed bilayers composed of bPC and bSM exhibit gel/fluid phase coexistence (Figs. 3 and 5, *A–D*). The observed gel fraction increases linearly as a function of the mole fraction of bSM (Fig. 6 *A*). We tested five different lipophilic fluorescent dyes, and all are excluded from the gel phase (Fig. 3). Cholesterol dramatically alters the nature of these membranes. The addition of only 5% cholesterol to bPC/bSM (1:1) bilayers leads to a decrease in the fraction of the fluid liquid-disordered (l_d) phase that is stained by all five dyes, the disappearance of corrugated gel phase domains, and the appearance of rounded domains that we ascribe to the liquid-ordered (l_o) phase (Fig. 3). Of the five dyes tested, only NBD-DPPE partitions favorably into the l_o phase (Fig. 3 *C*). This dye even allows us to view a case where three phases are present. At 5% cholesterol, the gel phase domains, which exclude the dye completely, and l_o phase domains, which incorporate more dye than the surrounding l_d phase, appear to coexist. At 20% cholesterol the gel phase is no longer visible, and the area fraction of the l_o phase domains is significantly higher. As cholesterol is increased to 35%, the NBD-DPPE partitions less completely into the l_o phase, and at 50% it appears to be equally distributed between the l_d and l_o phases. This indicates that the partitioning of NBD-DPPE into the l_o phase is not as favorable as the partitioning of the other dyes into the l_d phase, and that as cholesterol content is increased, the difference in the nature of the opposing phases is less pronounced.

Lateral diffusion measurements by FRAP support our interpretation of the images. As cholesterol is increased in 1:1 bPC/bSM bilayers from 0 to 20%, the fast fluorescence recovery fraction of the l_d phase (NBD-DOPE probe) increases from 25 to 67%. However, as cholesterol is further increased to 50%, the fast fluorescence recovery fraction

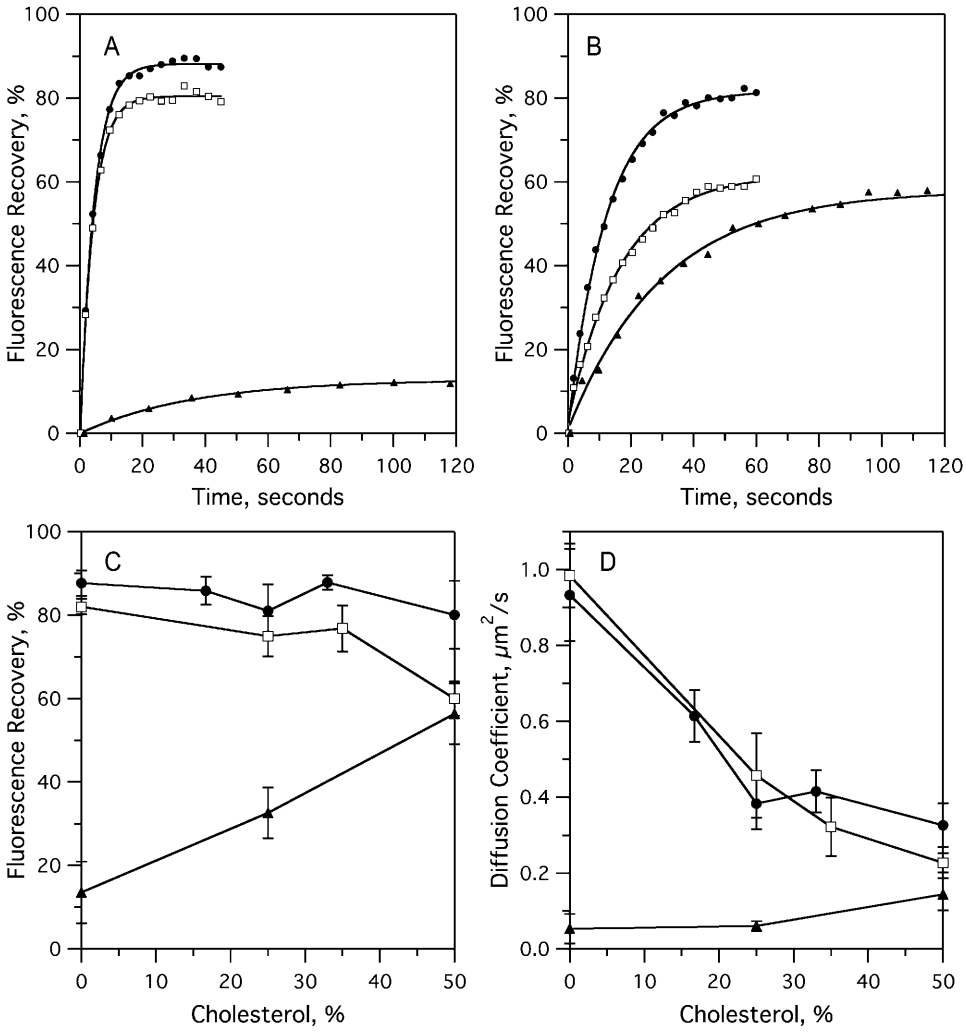

FIGURE 2 Fluorescence recovery after photobleaching (FRAP) experiments on bilayers of binary mixtures containing POPC, bPC, or bSM, and cholesterol. Bilayers were formed by the Langmuir-Blodgett/Schäfer method on quartz slides. Each bilayer was stained with 1% NBD-DOPE (NBD-DPPE in cases with bSM) in the monolayer applied distally to the quartz support. Experiments were performed at room temperature. (*A*) Examples of recovery curves in POPC (●), bPC (□), and bSM (▲) bilayers with no cholesterol. (*B*) Examples of recovery curves in POPC (●), bPC (□), and bSM (▲) bilayers with 50% cholesterol. (*C*) Fast fluorescence recovery fractions in POPC (●), bPC (□), and bSM (▲) bilayers as a function of cholesterol concentration. (*D*) Diffusion coefficients in POPC (●), bPC (□), and bSM (▲) bilayers as a function of cholesterol concentration. Each point in *C* and *D* is the mean ± SD of 12 curves obtained from at least three individually prepared bilayers.

decreases to 44%, indicating an increase in confinement of NBD-DOPE within the now discontinuous l_d phase (Fig. 4 *A*). In contrast, the fast fluorescence recovery fraction of the l_o phase (NBD-DPPE probe) increases continuously with cholesterol, as this phase occupies more of the membrane (Fig. 4 *A*). At 50% cholesterol, the observed fluorescence recovery is likely that of the entire membrane, because the dye partitions equally between the two phases (Fig. 3 *C*). At or below 5% cholesterol, the fluorescence of NBD-DPPE did not recover on the $\mu m^2/s$ length- and timescales, indicating a diffusion coefficient below our detection limit of 0.01 $\mu m^2/s$. At 20% cholesterol and above, both NBD-DOPE and NBD-DPPE had a diffusion coefficient of $\sim$0.2 $\mu m^2/s$ (Fig. 4 *B*).

The extracellular leaflet of the mammalian plasma membrane is composed of mostly PC, SM, and cholesterol. The PC/SM ratio varies depending on the cell type, from nearly equimolar (van Meer et al., 1981; Devaux, 1991) to over 3:1 (Friddriksson et al., 1999). We therefore examined the phase behavior at two different PC/SM ratios, namely 1:1 (Fig. 5, *E–H*) and 2:1 (Fig. 5, *I–L*). The fraction of the membrane in the l_o phase, as measured by the relative surface area of the dark regions in bilayers stained with Rh-DOPE, increases in both cases with cholesterol content. The contrast reverses between 20 and 25% cholesterol in the 1:1 mixture and between 25 and 30% cholesterol in the 2:1 mixture. Apparently, domains of l_o phase are included in a sea of l_d phase at the lower boundary concentration of cholesterol, whereas domains of l_d phase are included in a sea of l_o phase at the higher boundary concentration. The l_d phase becomes disconnected and the l_o phase becomes connected at the ''percolation'' threshold, which lies between 20 (25) and 25 (30)% cholesterol in the 1:1 (2:1) mixtures. In each case, the area fraction of l_o phase depends approximately linearly on the cholesterol concentration and is just $\sim$50% at the percolation threshold (Fig. 6, *B* and *C*).

One of the questions commonly asked about rafts is whether they span the entire membrane, or if they can also exist in only the inner or outer leaflet (van Meer, 2002). We examined symmetric preparations of bPC/bSM/cholesterol

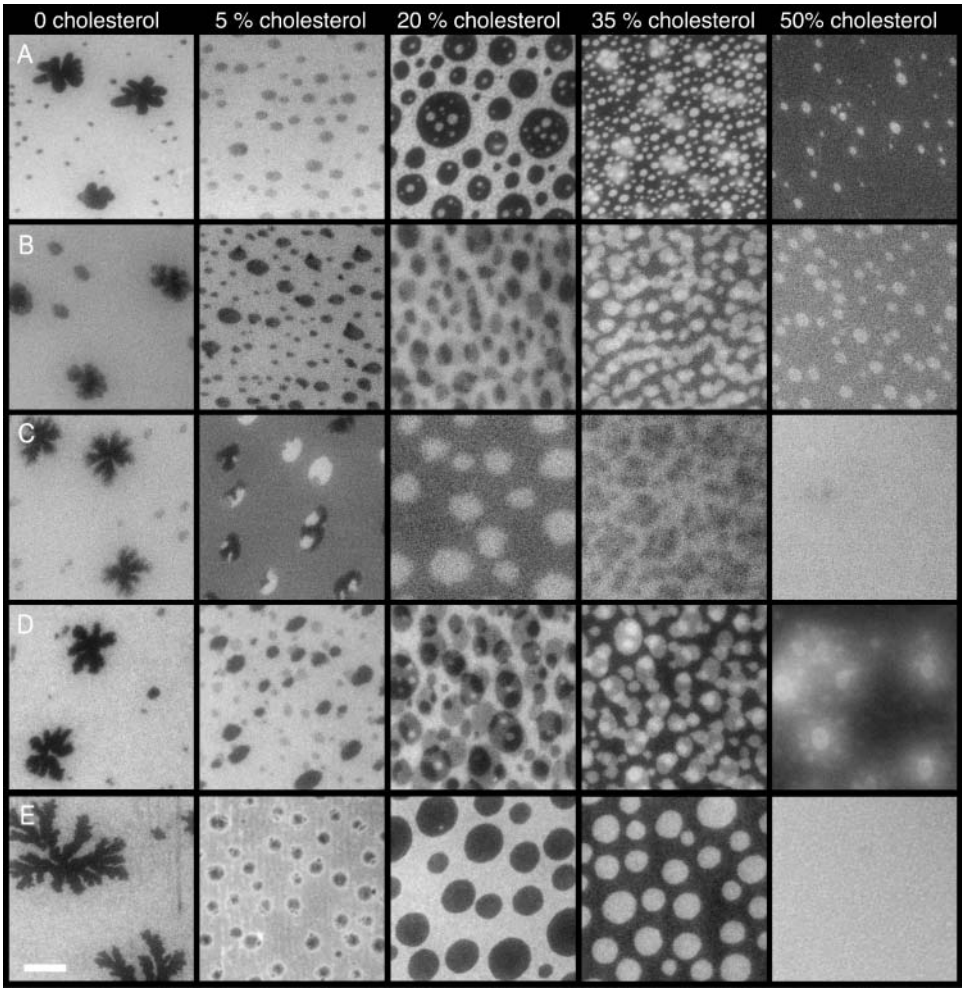

FIGURE 3 Fluorescence micrographs of bPC/bSM (1:1) bilayers with increasing cholesterol concentrations, and stained with various fluorescently labeled lipids. Bilayers were formed by the Langmuir-Blodgett/Schäfer method on quartz slides. Each bilayer was stained with the following dyes in the monolayer applied distally to the quartz support: (*A*) 0.5% Rh-DOPE, (*B*) 1% NBD-DOPE, (*C*) 1% NBD-DPPE, (*D*) 0.5% $DiIC_{12}$, and (*E*) 0.5% $DiIC_{18}$. Experiments were performed at room temperature. The white bar represents 10 μm.

in planar bilayers to see if the rafts lined up. In each experiment, only the monolayer that was applied distally to the support was stained, but in some cases the dye appears to flip across the membrane and stain both leaflets. The extent of the flipping depends on the dye used. In experiments with NBD-DOPE and $DiIC_{12}$, staining of both leaflets is observed in several images (Fig. 3, *B* and *D*). With Rh-DOPE, this is observed in only a few experiments (Fig. 3 *A*). With NBD-DPPE and $DiIC_{18}$, staining appears to be confined to the labeled outer leaflet (Fig. 3, *C* and *E*). The amount of the

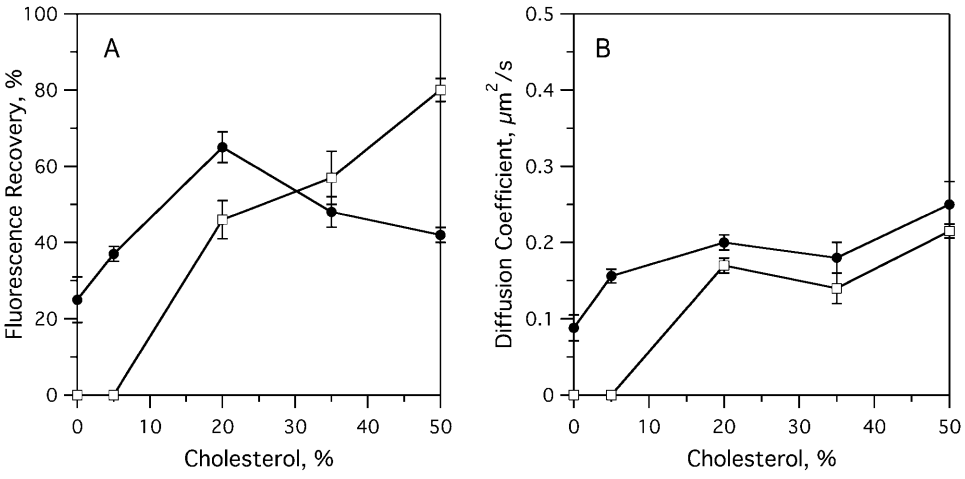

FIGURE 4 FRAP experiments on raft-containing planar bilayers with dyes that partition favorably into opposite phases. Bilayers were formed by the Langmuir-Blodgett/Schäfer method on quartz slides. Each bilayer was stained in the monolayer applied distally to the quartz support. Experiments were performed at room temperature. (*A*) Fast fluorescence recovery fractions in bPC/bSM (1:1) bilayers as a function of cholesterol concentration and stained with (●) 1% NBD-DOPE or (□) 1% NBD-DPPE. (*B*) Diffusion coefficients in bPC/bSM (1:1) bilayers as a function of cholesterol concentration and stained with (●) 1% NBD-DOPE or (□) 1% NBD-DPPE.

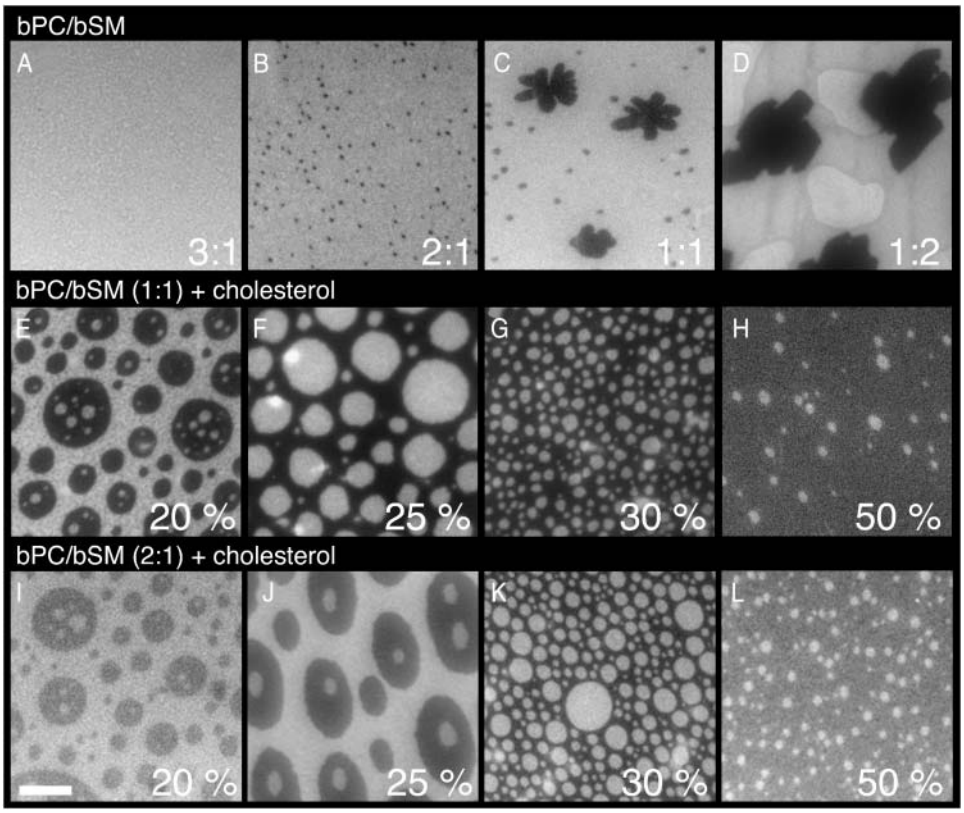

FIGURE 5. Fluorescence micrographs of bilayers at different bPC/bSM ratios and with different cholesterol concentrations. (*Top row*) bPC/bSM bilayers in ratios of *A*, 3:1; *B*, 2:1; *C*, 1:1; and *D*, 1:2, in the absence of cholesterol. (*Middle row*) bPC/bSM (1:1) with *E*, 20%; *F*, 25%; *G*, 30%; and *H*, 50% cholesterol. (*Bottom row*) bPC/bSM (2:1) with *I*, 20%; *J*, 25%; *K*, 30%; and *L*, 50% cholesterol. Bilayers were formed by the Langmuir-Blodgett/Schäfer method on quartz slides. Each bilayer was stained with 0.5% Rh-DOPE in the monolayer applied distally to the quartz support. Experiments were performed at room temperature. The white bar represents 10 μm.

other lipids that flip-flop between the two monolayers in supported bilayers is unknown, so we limited our studies to symmetric preparations with respect to PC, SM, and cholesterol. The extent of lipid flip-flop that occurs during and/or after the preparation of Langmuir-Blodgett/Schäfer bilayers will be the subject of a separate study. Regardless of the outcome of these experiments, several of the images in Fig. 3, *B* and *D*, indicate that l_o domains are not always correlated across the two leaflets in planar supported lipid bilayers.

Although separated from the membrane by a 1–2-nm water-filled cleft (Kiessling and Tamm, 2003), the solid substrate may still affect some aspects of the observed lipid domain behavior. To test whether the relative proportions of l_o and l_d phases are accurately represented in the planar bilayers, we developed a fluorescence resonance energy transfer (FRET) assay to measure the phase behavior in multilamellar liposomes of identical lipid compositions as used in the planar bilayer experiments. In these experiments, NBD-DOPE or NBD-DPPE were used as energy donors, and Rh-DOPE served as an energy acceptor. As shown in Fig. 7 *A*, NBD-DOPE and Rh-DOPE exhibit good spectral overlap, which makes this a suitable FRET pair. The R_0 was calculated, using Eqs. 4 and 5, from the spectra of Fig. 7 *A* and was found to be 52 $\pm$ 3 Å in pure bPC bilayers. We also measured NBD-DOPE emission and Rh-DOPE absorbance spectra in liposomes prepared from a l_o phase 1:1 bSM/cholesterol mixture. Although there were minor differences between these and the corresponding spectra of Fig. 7 *A* (data not shown), the R_0 calculated from these spectra was still 53 $\pm$ 3 Å, i.e., the same as in l_d phase lipids.

The efficiency of fluorescence energy transfer in a single-phase homogeneous membrane can be calculated as a function of the overall dye density, donor/acceptor ratio, and R_0. The solution takes the form (Wolber and Hudson, 1979) of

$$E = 1 - \int_0^\infty \exp(-t/\tau - 4.25409\,R_0^2\,cP_a(t/\tau)^{1/3})dt, \quad (7)$$

where t is time, τ is the lifetime of an excited donor in the absence of acceptors, c is the concentration of dyes per unit area, and P_a is the fraction of dyes that are acceptors. For all calculations reported here, $c = C/A$ was given by the total concentration of both dyes in units of mole fraction, C, and the surface area per lipid in the membrane, A, which was taken to be 70 Å^2 for phospholipids in the l_d phase (Lewis and Engelman, 1983). Thus, Eq. 7 allows one to calculate E versus P_a curves without any free parameters. To check the validity of this approach, we compared calculated E versus P_a curves with experimentally determined ones for C ranging from 0.2 to 2% in pure bPC bilayers in the l_d phase. Fig. 7 *C* shows ''perfect'' superpositions of theory and experiment at total dye concentrations of 0.5 and 1%. At 0.2% total dye, the

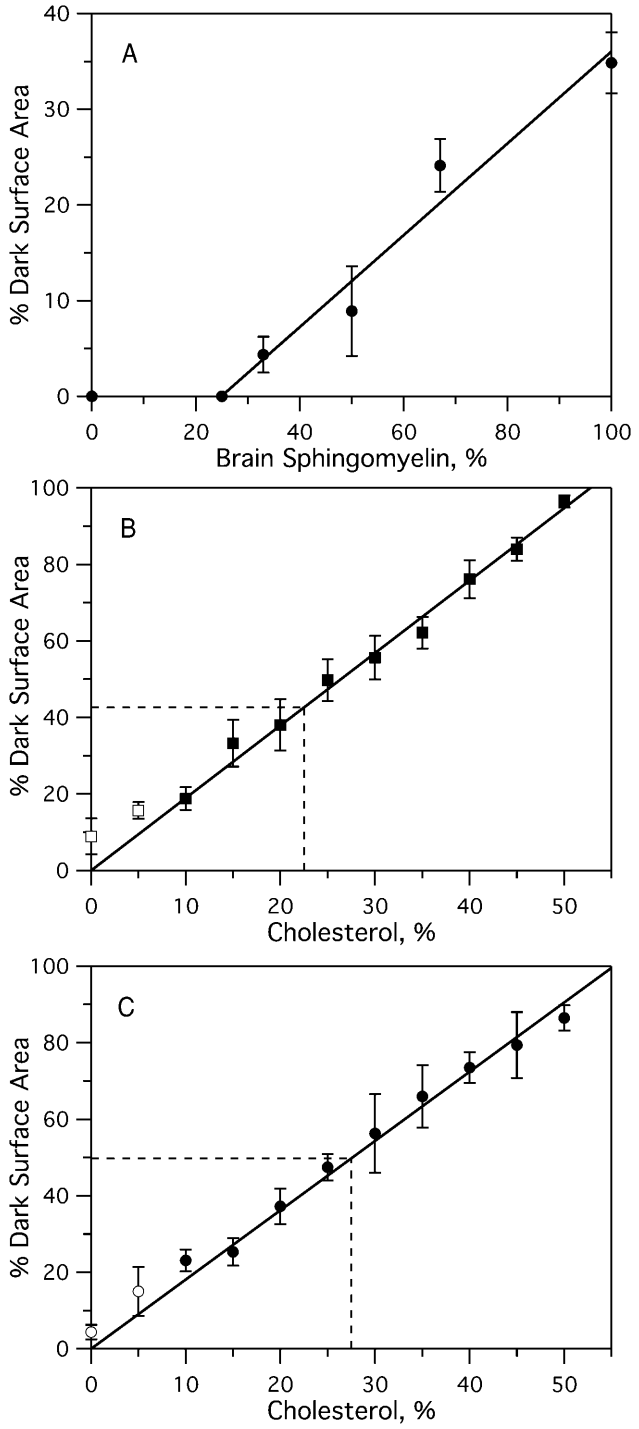

FIGURE 6 Percent dark surface area as a function of bPC, bSM, or cholesterol as determined by analyzing the fluorescence images of planar lipid bilayers formed by the Langmuir-Blodgett/Schäfer method on quartz slides. Each bilayer was stained with 0.5% Rh-DOPE in the monolayer applied distally to the quartz support. Experiments were performed at room temperature. (*A*) Percent dark area as a function of percent bSM in binary bPC/bSM mixtures (from Fig. 5, *A–D*). The line represents the least-squares fit of the data above 25% SM. (*B* and *C*) Percent dark area versus cholesterol content (*B*) 1:1 bPC/bSM (from Fig. 5, *E–H*) and (*C*) 2:1 bPC/bSM (from Fig. 5, *I–L*). Solid lines represent a least-squares fit through the origin. Points representing 0 and 5% cholesterol were excluded from the fit because the dark areas represent gel (0% cholesterol) and a mixture of gel and l_o phases (5% cholesterol, see text). Dashed lines represent approximate locations of the percolation threshold.

data are relatively noisy so that no definite conclusion about the agreement between theory and experiment can be reached, whereas at 2%, the theoretical model appears to break down. Least-squares fitting of the data to Eq. 7 (*dashed lines*) gives values for C of 0.15 at 0.2%, 0.99 at 1%, 0.50 at 0.5%, and 1.77 at 2% total dye (Fig. 7 *C*). This analysis shows that total dye concentrations can be accurately determined by this method, if the total dye concentrations are in the 0.5–1% range. NBD-DOPE and NBD-DPPE work equally well as energy donors in single-phase fluid lipid bilayers. We also analyzed our data with the two-dimensional Perrin equation (Eq. 1 of Chattopadhyay and London, 1987; with a 9.4 Å closest approach between two lipids) and as expected, found essentially the same result as with the Wolber-Hudson model. We also extended the Perrin equation to include possible FRET between probes in different leaflets of the lipid bilayer. These theoretical curves lie ~15–20% above those shown in Fig. 7 *C* and therefore underestimate the actual dye concentrations in the bilayers (data not shown). The reason for this unexpected result is unknown, but may be due to two errors (e.g., neglect of transbilayer quenching and a systematic error in the determination of R_0, which requires input of a crudely estimated dipole orientation factor) that fortuitously compensate and therefore yield the extremely good agreement between theory and experiment. Regardless, Fig. 7 *C* shows that the Wolber-Hudson model is sufficient and can be used to accurately determine dye concentrations in lipid bilayers.

Having established that the concentration of dyes in lipid bilayers can be reliably determined by FRET, we proceeded to use this technique to measure phase separations in mixed lipid systems. In a first set of experiments, NBD-DOPE and Rh-DOPE (0.5% total) were incorporated into model membranes composed of bPC/bSM (1:1) with 35% cholesterol. Our imaging experiments had shown that bilayers of this mixture contain 62% l_o phase and 38% l_d phase lipid (Fig. 6 *B*), and that NBD-DOPE and Rh-DOPE partition favorably into the l_d phase (Fig. 3, *A* and *B*). As expected for a phase-separated bilayer, the FRET efficiency increased due to exclusion of both dyes from the l_o phase and their confinement to a smaller area of l_d phase lipid (Fig. 8). In additional FRET experiments, NBD-DPPE was used as a donor, with Rh-DOPE as the acceptor. In this case, the donor and acceptor dyes partition into opposing phases (Fig. 3, *A* and *C*). This was confirmed by a lower observed transfer efficiency than in the single-phase bPC bilayers (Fig. 8). FRET measurements of the temperature-dependence of the l_o/l_d phase separation indicate that l_o phase rafts persist up to temperatures of at least 50°C, but melt somewhere below 70°C in the 1:1 bPC/bSM-plus-35% cholesterol system.

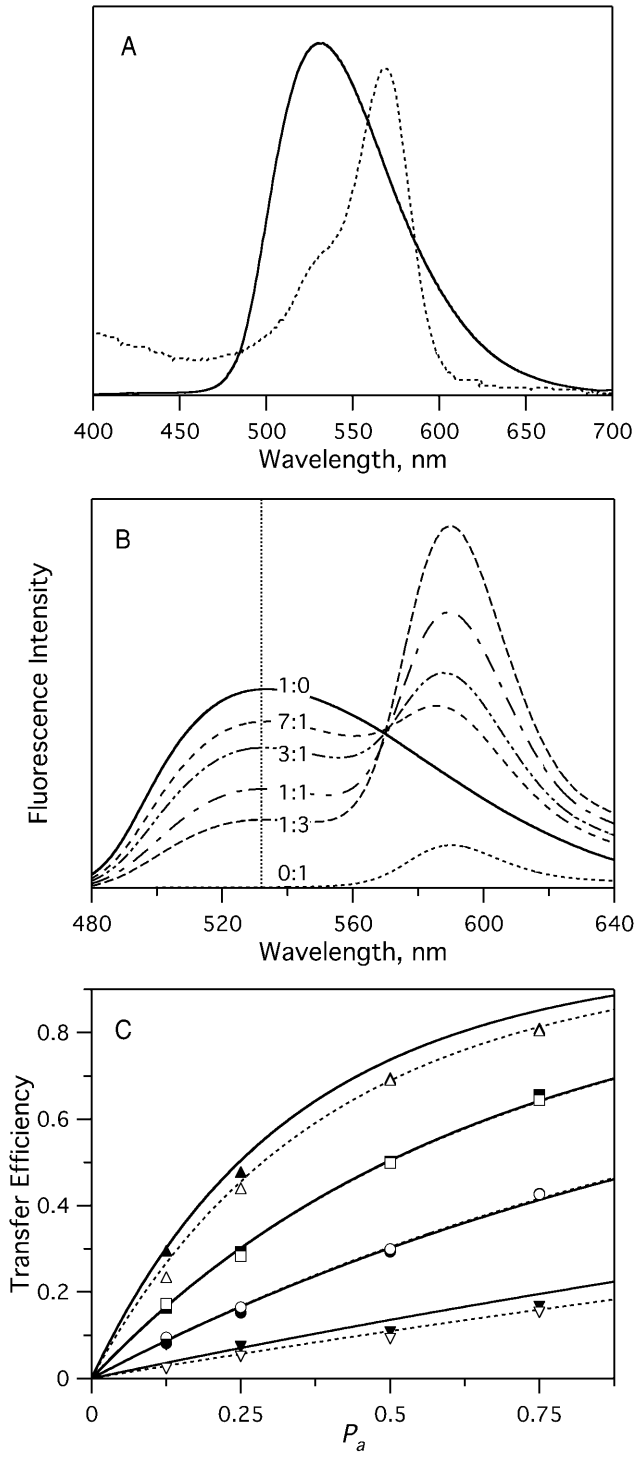

FIGURE 7 FRET between NBD-PE and Rh-DOPE in multilamellar liposomes of pure bPC. (*A*) Spectral overlap of NBD-DOPE emission (*solid*) and Rh-DOPE absorbance (*dashed*). Dye concentration was 1% of the total lipid in both cases. (*B*) Example of a FRET experiment. Emission spectra with labels indicating the NBD-DOPE/Rh-DOPE ratio. Total dye concentration was 1%. Intensities were normalized to emission at 532 nm in the presence of 50 mM β-OG, where all FRET was relieved. (*C*) Comparison of experimental results to the model of Wolber and Hudson (1979). The plots show FRET efficiency versus P_a (mole fraction of dyes that are acceptors) in bPC vesicles with (▼,▽) 0.2%, (●,○) 0.5%, (■,□) 1%, and (▲,△) 2% dye. (For *solid symbols*, NBD-DOPE was the donor; for *open symbols*, NBD-DPPE was the donor.) Rh-DOPE was the acceptor in every case. Solid curves are calculated transfer efficiencies using known dye concentrations and Eq. 7. Dashed curves are least-squares fits of the experimental data to Eq. 7. Excitation was at 466 nm. All experiments were performed at 25°C.

These results are consistent with earlier fluorescence experiments using nitroxide quenchers in a similar lipid system (Ahmed et al., 1997; Wang et al., 2000; Xu and London, 2000).

The observed energy transfer in a membrane of two coexisting phases should behave as follows (London and Feigenson, 1981),

$$E_{obs} = f_{ld}E_{ld} + f_{lo}E_{lo}, \tag{8}$$

where f_i is the fraction of dyes that partition into the i phase and E_i is the transfer efficiency within that phase, as described by Eq. 7. For analysis using this relationship, we consider only the system with DOPE-linked dyes. If we know the ratio of the amount of dyes in the l_d phase to the amount of dyes in the l_o phase, Q, such that

$$f_{ld} = \frac{Q}{1+Q} \quad \text{and} \quad f_{lo} = \frac{1}{1+Q}, \tag{9}$$

then we can fit the data to this model to find c_{ld} and c_{lo}, the concentration of dyes in the l_d and l_o phases, respectively. We can then determine the fraction of the membrane in each phase X_{ld} and X_{lo} by

$$X_{ld} = \frac{c_0}{c_{ld}} f_{ld} \quad \text{and} \quad X_{lo} = 1 - X_{ld}, \tag{10}$$

where c_0 is the concentration of dyes in the single-phase membranes. The fitting equation can be reduced to solve for only one concentration, c_{ld}, because c_{lo} is restricted by conservation of mass:

$$c_{lo} = \frac{c_0(1-f_{ld})}{1-X_{ld}}. \tag{11}$$

Fig. 9 *A* shows an analysis of the results from the experiments of Fig. 8 *A* with the raft-producing 1:1 bPC/bSM-plus-35% cholesterol mixture at 25°C, assuming various values of Q. The calculated fraction of the membranes in the l_o phase increases from ~30–70% when Q decreases from ∞ to 2 (Fig. 9 *A*). We can estimate the partition coefficient for dye partitioning between the two phases, K_p, from the relative fluorescence intensities of the l_d and l_o phases in the images of the planar bilayers of Fig. 3, *A* and *B*, and find $K_p = 3.1 \pm 0.5$ for NBD-DOPE and $K_p = 4.8$

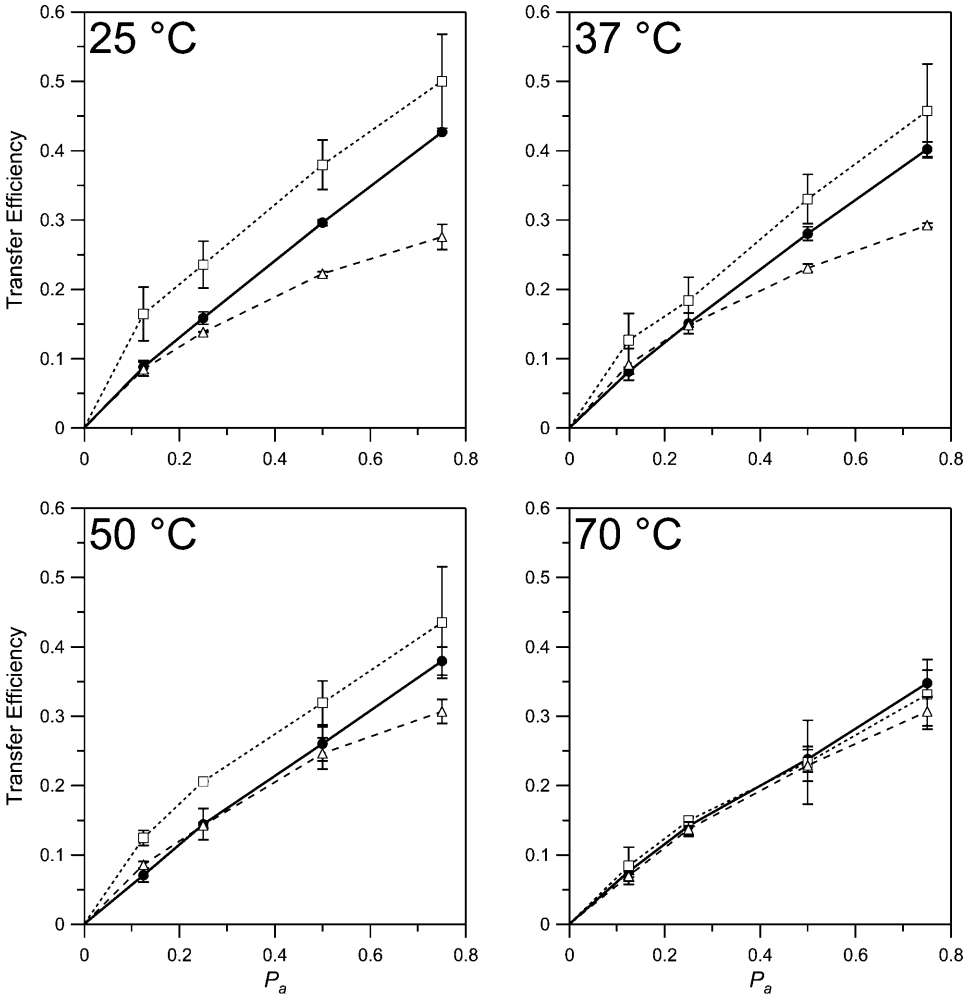

FIGURE 8 Comparison of transfer efficiencies in the presence and absence of rafts. ● are from bPC bilayers in multilamellar liposomes in the absence of cholesterol and at a dye concentration of 0.5% in bPC, with a donor of NBD-DPPE or NBD-DOPE and an acceptor of Rh-DOPE. □, bPC/bSM (1:1), 35% cholesterol, 0.5% NBD-DOPE/Rh-DOPE. △, bPC/bSM (1:1), 35% cholesterol, 0.5% NBD-DPPE/Rh-DOPE.

± 0.7 for Rh-DOPE. To estimate these values of K_p we subtracted intensities of the fingered gel phase domains as backgrounds, assuming that the two probes do not partition into gel phases. Since the area fraction of l_o phase in these images is 62 ± 4% (Fig. 6 *B*), we calculate that $Q = K_p \times (38/62) = 1.9 \pm 0.4$ and 2.9 ± 0.6, for the two dyes, respectively. The value of especially NBD-DOPE is probably an underestimate because of some photobleaching during image acquisition. Therefore, our best estimates for K_p and Q of both dyes are 5 and 3, respectively. Using $Q = 3$, we find from the data of Fig. 9 *A* that 60 ± 5% of the total membrane comprises l_o phase lipid in the multilamellar liposomes. This fraction is the same as the 62 ± 4% found by simple area analysis of the images of planar bilayers of the same lipid composition. We estimate the error of this analysis of fractional l_o phase areas in multilamellar liposomes not to exceed 15%. For example, if K_p were underestimated by a drastic 50% and were 7.5 instead of 5, Q would become 4.6 and the l_o phase area would be 52%, which is only 13% smaller than our best estimate. Therefore, we believe that measurements of area fractions of the l_o phase in planar supported bilayers (Fig. 6) correspond quite closely to the areas of l_o phase lipid in multilamellar liposomes under identical conditions. This does not mean that the sizes of the observed domains in are also representative of those occurring in the liposomes. The FRET method as employed here cannot be used to determine domain sizes in the multilamellar liposomes. Although it is easy to observe the domains directly in the planar supported membranes, the liposomes offer the advantage that temperature is more easily controlled. The l_o phase fractions in liposomes were calculated from the data of Fig. 8 and found to be 45–60% at 37 and 50°C, respectively (Fig. 9 *B*). As noted before, rafts melt above 50°C and the bilayers exhibit only l_d phase lipid at 70°C.

DISCUSSION

We have shown that supported planar lipid bilayers can be successfully employed to measure the effect of cholesterol on the domain organization and dynamic properties of PC,

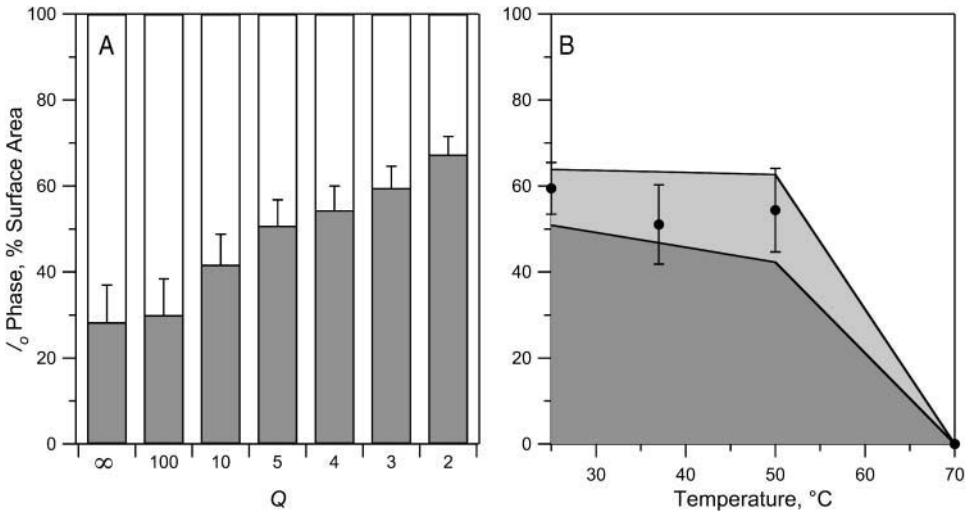

FIGURE 9 Area fractions of l_o phase lipid calculated from the data presented in Fig. 8 using Eqs. 8 and 10. (*A*) Area fraction of l_o phase as a function of the ratio Q of DOPE-linked dyes in the l_d phase divided by DOPE-linked dyes in the l_o phase at 25°C. (*B*) Area fraction of l_o phase as a function of temperature, assuming $Q = 3$. The lighter shaded area represents the area of uncertainty as delineated by least-squares fits to the extrema of the error bars of the first three data points.

SM, and mixed PC/SM bilayers. An important conclusion from our studies is that we obtain the same area fraction of lipids in the l_o phase in supported planar bilayers by direct visualization and image analysis as by FRET analysis in multilamellar liposomes of identical composition. The planar bilayer geometry offers several advantages over more conventional lipid model membranes:

1. Domains of different lipid phases can be directly observed and there is no ambiguity in the interpretation of the partitioning of fluorescently labeled molecules, i.e., lipids or proteins, between the various lipid phases.
2. FRAP experiments to measure lateral diffusion of membrane components are readily carried out in planar model membranes and allow one to characterize the nature and dynamic properties of the phases that are present in the sample.
3. Single molecules can be identified and their paths of lateral motion can be tracked under appropriate conditions. Single molecule techniques should be helpful to further characterize the properties of the coexisting lipid phases and, more importantly, will be helpful to monitor the behavior of selected molecules in an environment of coexisting lipid phases.
4. It should be possible to make planar bilayers with asymmetric lipid distributions that mimic the lipid asymmetry in cell membranes, thus beginning to address the question of how raft-forming domains of different lipid compositions are coupled across the two leaflets of asymmetric lipid bilayers.

Despite these advantages, there are caveats about some aspects of the observed domains in planar supported lipid bilayers. Although our comparisons with multilamellar liposomes yield the same l_o phase area fractions in planar bilayers, it is not yet clear whether the sizes and shapes of the domains that are observed in planar model membranes accurately reflect those present in spherical model membranes or cell membranes. Large circular domains of l_o phase lipids have been observed in giant unilamellar vesicles composed of raft lipid components (Dietrich et al., 2001a; Veatch and Keller, 2002; Kahya et al., 2003; Baumgart et al., 2003). The sizes of these domains are comparable to those observed in our planar membranes. However, l_o phase domains are sometimes slightly elliptical in planar bilayers as if they had been stretched by the direction of the Langmuir-Blodgett deposition of the first (unstained) lipid layer. The implication of this observation is that the domains are not totally uncoupled from the solid support although a water-filled gap of ~2 nm exists between the silicon oxide surface and the headgroups of the first monolayer (Kiessling and Tamm, 2003) and although the lipids in both leaflets of the bilayer are freely mobile (Tamm, 1988). It is possible that supported bilayers are ''pinned'' at individual point defects or rough spots that protrude from the silicon oxide surface. This would hold the domains stretched and in place in the planar membrane system, although they are free to laterally move as a whole and to adopt shapes (circles) with minimal linear interface between domains of the different lipid phases in spherical model membranes. Unfortunately, we were so far unsuccessful in attempts to image domains in polyethylene-glycol-supported bilayers, which are more uncoupled from the silicon oxide surfaces than directly supported bilayers (Wagner and Tamm, 2000; Kiessling and Tamm, 2003). The sizes and shapes of domains in multilamellar liposomes are not known and l_o phase domains (''rafts'') have never been directly visualized in cell membranes. It is possible that because of the high complexity of cell membranes, rafts are much smaller, i.e., beyond the resolution of the light microscope in living systems (see Edidin, 2003, for a contemporary critical review on the relation of findings in cell and model membranes). In conclusion, we believe that the planar raft model membrane

system presented here is useful to measure partitioning and motional properties of membrane components in membranes of defined and perhaps even asymmetric lipid (and protein) composition, but that one should be careful about drawing far-reaching conclusions from the sizes and shapes of the domains seen in these images.

The lateral diffusion measurements by FRAP reported in Figs. 2 and 4 provide useful information toward an initial characterization of the dynamic properties of the lipid mixtures that were investigated in this study. Whether liquid-ordered, liquid-disordered, or both, a fluid lipid bilayer should have a total fluorescence recovery of 100%, and indeed, even a gel phase bilayer should have a recovery of 100% if probed over a long enough time. In samples with coexisting phases one might therefore generally expect superimposed recoveries on different timescales. However, long acquisition times cannot be used in pattern photobleaching to simultaneously record two vastly different diffusion coefficients because dyes from outside the circular observation area will enter, rendering Eq. 1 invalid. Therefore, we restricted ourselves to only recording the fastest components in each sample and the percentage of recoveries are reported for these components only. It should also be noted that FRAP curves of these components generally gave good fits to single exponentials as expected from Eq. 1 for a single component. Deviations from 100% recovery in FRAP experiments may be due to a number of factors, including two-component diffusion with a slow component that is too slow to observe on the experimental timescale, or immobilization of lipids in defects on the glass surface. For an analysis of these data, it is also important to realize that lateral diffusion measurements on membranes with heterogeneous structures depend on the lengthscale over which the experiment is conducted and on the relative partitioning of the probe molecule into coexisting phases. We measured FRAP by pattern photobleaching with stripe widths of 6.3 and 4.0 (most experiments) and 1.6 μm (experiments with samples that exhibited slow diffusion; e.g., NBD-DPPE in bSM or bSM:cholesterol or ternary lipid mixtures at low cholesterol). Therefore, our experiments pertain to relatively long-range lateral diffusion. Lateral diffusion in a heterogeneous system may be faster and less restricted if probed over shorter distances. We first discuss the data of the binary systems presented in Fig. 2: Since no lateral heterogeneity has been observed in the POPC and bPC bilayers at any concentration of cholesterol (except for the unusual case of 50% in bPC that was discussed above), the observed diffusion behavior is likely that of single phases in each of these cases. Cholesterol decreases the diffusion coefficient of NBD-DOPE up to threefold in POPC and bPC. Although their absolute diffusion coefficients are larger, the same relative decrease has been reported by Kahya et al. (2003), who measured lateral diffusion on a lengthscale of $\sim$0.4 μm by fluorescence correlation spectroscopy (FCS) in giant unilamellar vesicles. In planar bilayers of bSM, NBD-DPPE diffusion is low and increases slightly as cholesterol is increased. As discussed above, these membranes probably consist of submicroscopic domains with NBD-DPPE trapped between them. The diffusion results may be explained if increasing amounts of the trapped dyes are released as the cholesterol concentration is increased in these bilayers. These data are also in good qualitative agreement with FCS data on a similar lipid system in giant vesicles (Kahya et al., 2003).

More dyes diffuse on the micrometer lengthscale in ternary than in binary lipid mixtures with bSM when the cholesterol concentration is increased (Fig. 4). However, these experiments are complicated by the fact that 1–10 μm-sized domains are present in these mixtures. Therefore, it is not surprising that different results are obtained when NBD-DOPE, which partitions preferentially into l_d phases, and NBD-DPPE, which partitions preferentially into l_o phases, are used in these experiments. Diffusion (fast recovery fraction and coefficient) of NBD-DOPE increases up to 20% cholesterol. The fast fluorescence recovery fraction decreases above this point because the l_d phase becomes disconnected at higher cholesterol concentrations. The fast recovery fraction above the percolation threshold is not zero because some photobleached stripes cross the l_d domains and because increasing fractions of NBD-DOPE are forced into the l_o phase as the l_d phase becomes rare. Diffusion of the ''l_o probe'' NBD-DPPE is much lower than that of NBD-DOPE at low cholesterol. Although NBD-DPPE preferentially stains the l_o phase, its partitioning into that phase is weak and it eventually no longer favors l_o over l_d phases at high cholesterol (see Fig. 3 *C*). Therefore, the observed diffusion is dominated at low cholesterol by that of the (disconnected) l_o phase and gradually moves toward representing diffusion of the connected l_o phase and the disconnected l_d phase at 50% cholesterol. We wish to emphasize that our diffusion experiments are not intended to obtain a detailed molecular picture of the dynamic behavior of the molecules in each phase. However, we believe they provide a useful qualitative insight into the diffusive behavior of the molecules in these mixtures. Clearly, measurements of diffusion by single particle tracking, where particles can be assigned to reside in individual phases, give a much more detailed and accurate view of the diffusive behavior of these molecules. Such an experiment has been carried out in supported monolayers of similar composition (Dietrich et al., 2001a,b). These authors found an approximately threefold reduction of the diffusion coefficient when a labeled lipid entered a l_o phase domain from a l_d phase domain. Consistent with these and our results, Kahya et al. (2003) also observed smaller diffusion coefficients in l_o phase domains than in coexisting l_d phase domains and a merging of the diffusive behavior of the two phases at high cholesterol. Because FCS measures local diffusion of fewer molecules in clearly assigned domains, differences of the diffusion behavior in the two phases are much more clearcut than in our case where we average over

many more molecules and incur some contamination from signals of opposing phases.

A striking result of our studies is the linear relationship of the area fraction of l_o phase domains as a function of cholesterol concentration at two PC/SM ratios (Fig. 6). Very importantly, both lines reach 100% dark, i.e., full conversion to a single l_o phase at relatively high cholesterol concentrations of ~50 and 55%, respectively. Since at these points the bPC/bSM contents are 25:25 and 30:15, respectively, and since the maximum solubility of cholesterol in phospholipids (and probably also sphingolipids) is 66% (Huang et al., 1999), it is immediately clear that l_o phase domains close to these points cannot be composed of only bSM and cholesterol, but must also contain substantial fractions of bPC. This notion is supported by fluorescence quenching data in similar ternary lipid mixtures as those investigated here, indicating that in addition to the major SM fraction (Wang and Silvius, 2003), substantial fractions of monounsaturated phospholipids also partition into the l_o phases (Wang et al., 2000). Although the area fraction of l_o phase changes linearly with cholesterol concentration, the observed trajectories cannot be tie lines through the l_o–l_d coexistence region of the ternary phase diagram because 1), The diffusion coefficient of lipid tracers in the l_o phase increases 10-fold as the cholesterol concentration is increased from 10 to 50% in a 1:1 PC/SM mixture (Kahya et al., 2003) and 2) Fig. 3 *C* shows that the coefficient of NBD-DPPE partitioning between l_o and l_d phase domains changes substantially as the cholesterol concentration changes in the two-phase region of the 1:1 bPC/bSM mixture. Both observations provide convincing evidence that the compositions and physical properties of the two phases change along the cholesterol concentration axis at 1:1 and 2:1 bPC/bSM in the ternary phase diagram.

These and previous observations that PCs are quite prevalent in l_o phase domains seems to contradict the well-established fact that cell membranes extracted with cold Triton X-100 are enriched in cholesterol and SM whereas PCs and other unsaturated lipids are extracted. We think that this behavior is an artifact of the detergent extraction method and that the selective interaction is induced or at least greatly amplified by the detergent. Strong evidence for this possibility comes from Heerklotz (2002) who showed by calorimetry and ^{31}P-NMR that Triton X-100 at low concentrations creates l_o phases in raft lipid mixtures. At higher concentrations, Triton X-100 extracts micelles (presumably consisting mostly of PCs) and leaves behind pure l_o phase bilayers (presumably consisting mostly of SMs and cholesterol) in these model studies. The separation of lipids by detergent extraction is therefore not representative of the lipid compositions in l_o and l_d phases in lipid bilayer membranes.

The percolation threshold where l_o phase domains become connected and l_d phase domains become disconnected occurs at a point where ~47% of the total membrane area has been converted into the l_o phase. In 1:1 bPC/bSM bilayers, this occurs between 20 and 25% cholesterol; and in 2:1 bPC/bSM bilayers, the transition falls between 25 and 30% cholesterol (Fig. 5). Since the transition appears to occur at roughly the same area fraction at both PC:SM ratios, we suspect that this point is independent of the actual domain size and shape and may therefore also occur at this area fraction in liposomes and cells where we cannot directly see the domains. If a percolation point indeed exists in cells as observed here, it could have far-reaching biological consequences. By only tweaking the cholesterol concentration or the PC/SM ratio slightly, the cell membrane could undergo a transition between two states in which completely different sets of proteins, i.e., raft and nonraft proteins, would become connected and able to react with one another by a lateral diffusion process (Thompson et al., 1995). It is interesting to note that the physiological concentration of cholesterol in mammalian cell membranes is on the order of 35 mol %, i.e., at a concentration where the l_o phase should be connected at both PC:SM ratios at room temperature. However, at 37°C and 35 mol % cholesterol, we estimate the raft area fraction to be reduced to ~50% (Fig. 9), i.e., again very close to our observation of the critical threshold area fraction for the percolation transition. Therefore, small changes in metabolic rates of lipid synthesis and breakdown and cholesterol homeostasis could indeed have profound physiological consequences on the rates of reactions between membrane components.

Using planar model membranes to study lipid rafts has advantages, in that the lipid composition can be controlled exactly and the observed phases can be attributed to the various properties of the lipids in the system. The system should also be well suited to measure the distribution and individual motional properties of membrane proteins, as Jacobson and co-workers have already demonstrated with lipid-anchored membrane proteins in supported monolayers (Dietrich et al., 2001b; Kahn et al., 2003). An interesting question will be to ask to what extent integral membrane proteins perturb raft formation. It is unlikely that they perturb the formation of cholesterol-lipid complexes, but they may well affect the cooperativity of the lateral phase separation of complexes into large rafts. High concentrations of perturbing membrane proteins could reduce rafts to the assembly of just a few cholesterol-lipid complexes in cell membranes—which, however, may still selectively trap some, but not all, membrane proteins. Such trapping and additional interactions of certain membrane proteins and protein-lipid complexes with the cytoskeleton may be responsible for the observation of small confinement zones when the motions of individual lipids and proteins are tracked in cell membranes by single molecule techniques (Schütz et al., 2000; Pralle et al., 2000; Dietrich et al., 2002). We believe that model membranes, spherical or planar, amplify some of the underlying membrane heterogeneity that is also present in cell membranes and therefore provide a useful additional window to study lipid-lipid and lipid-protein interactions in such membranes. The reconstitution approach will hopefully guide us to

a deeper future understanding of raft interactions in cell membranes.

This work was supported by grant AI30557 from the National Institutes of Health.

REFERENCES

Ahmed, S. N., D. A. Brown, and E. London. 1997. On the origin of sphingolipid/cholesterol-rich detergent-insoluble cell membranes: physiological concentrations of cholesterol and sphingolipid induce formation of a detergent-insoluble, liquid-ordered phase in model membranes. *Biochemistry.* 36:10944–10953.

Anderson, R. G. W., and K. Jacobson. 2002. A role for lipid shells in targeting proteins to caveolae, rafts, and other lipid domains. *Science.* 296:1821–1825.

Baird, B., E. D. Sheets, and D. Holowka. 1999. How does the plasma membrane participate in cellular signaling by receptors for immunoglobulin E? *Biophys. Chem.* 82:109–119.

Baumgart, T., T. S. Hess, and W. W. Webb. 2003. Imaging coexisting fluid domains in biomembrane models coupling curvature and line tension. *Nature.* 425:821–824.

Bloch, K. 1991. Cholesterol: evolution of structure and function. *In* Biochemistry of Lipids, Lipoproteins and Membranes. D. E. Vance and J. E. Vance, editors. Elsevier, Amsterdam, The Netherlands. 363–381.

Brown, D. A., and E. London. 2000. Structure and function of sphingolipid- and cholesterol-rich membrane rafts. *J. Biol. Chem.* 275:17221–17224.

Brown, D. A., and J. K. Rose. 1992. Sorting of GPI-anchored proteins to glycolipid-enriched membrane subdomains during transport to the apical cell surface. *Cell.* 68:533–544.

Chattopadhyay, A., and E. London. 1987. Parallax method for direct measurement of membrane penetration depth utilizing fluorescence quenching by spin-labeled phospholipids. *Biochemistry.* 26:39–45.

Connor, J., and A. J. Schroit. 1987. Determination of lipid asymmetry in human red cells by resonance energy transfer. *Biochemistry.* 26:5099–5105.

Devaux, P. F. 1991. Static and dynamic lipid asymmetry in cell membranes. *Biochemistry.* 30:1163–1173.

Dietrich, C., L. A. Bagatolli, Z. N. Volovyk, N. L. Thompson, M. Levi, K. Jacobson, and E. Gratton. 2001a. Lipid rafts reconstituted in model membranes. *Biophys. J.* 80:1417–1428.

Dietrich, C., Z. N. Volovyk, M. Levi, N. L. Thompson, and K. Jacobson. 2001b. Partitioning of Thy-1, GM1, and cross-linked phospholipid analogs into lipid rafts reconstituted in supported model membrane monolayers. *Proc. Natl. Acad. Sci. USA.* 98:10642–10647.

Dietrich, C., B. Yang, T. Fujikawa, A. Kusumi, and K. Jacobson. 2002. Relationship of lipid rafts to transient confinement zones detected by single particle tracking. *Biophys. J.* 82:274–284.

Edidin, M. 2003. The state of lipid rafts: from model membranes to cells. *Annu. Rev. Biophys. Biomol. Struct.* 32:257–283.

Feigenson, G. W., and J. T. Buboltz. 2001. Ternary phase diagram of dipalmitoyl-PC/dilauroyl-PC/cholesterol: nanoscopic domain formation driven by cholesterol. *Biophys. J.* 80:2775–2788.

Friddriksson, E. K., P. A. Shipkova, E. D. Sheets, D. Holowka, B. Baird, and F. W. McLafferty. 1999. Quantitative analysis of phospholipids in functionally important membrane domains from RBL-2H3 mast cells using tandem high-resolution mass spectrometry. *Biochemistry.* 38:8056–8063.

Heerklotz, H. 2002. Triton promotes domain formation in lipid raft mixtures. *Biophys. J.* 83:2696–2701.

Huang, J., J. T. Buboltz, and G. W. Feigenson. 1999. Maximum solubility of cholesterol in phosphatidylcholine and phosphatidylethanolamine bilayers. *Biochim. Biophys. Acta.* 1417:89–100.

Hwang, J., L. K. Tamm, C. Böhm, T. S. Ramalingam, E. Betzig, and M. Edidin. 1995. Nanoscale complexity of phospholipid monolayers investigated by near-field scanning optical microscopy. *Science.* 270:610–614.

Kahn, T. K., B. Yang, N. L. Thompson, S. Maekawa, R. M. Epand, and K. Jacobsen. 2003. Binding of NAP-22, a calmodulin-binding neuronal protein, to raft-like domains in model membranes. *Biochemistry.* 42:4780–4786.

Kahya, N., D. Scherfeld, K. Bacia, B. Poolman, and P. Schwille. 2003. Probing lipid mobility of raft-exhibiting model membranes by fluorescence correlation spectroscopy. *J. Biol. Chem.* 278:28109–28115.

Kalb, E., S. Frey, and L. K. Tamm. 1992. Formation of supported planar bilayers by fusion of vesicles to supported phospholipid monolayers. *Biochim. Biophys. Acta.* 1103:307–316.

Kiessling, V., and L. K. Tamm. 2003. Measuring distances in supported bilayers by fluorescence interference contrast microscopy: polymer supports and SNARE proteins. *Biophys. J.* 84:408–418.

Lewis, B. A., and D. M. Engelman. 1983. Lipid bilayer thickness varies linearly with acyl chain length in fluid phosphatidylcholine vesicles. *J. Mol. Biol.* 166:211–217.

London, E., and D. A. Brown. 2000. Insolubility of lipids in Triton X-100: physical origin and relationship to sphingolipid/cholesterol membrane domains (rafts). *Biochim. Biophys. Acta.* 1508:182–195.

London, E., and G. W. Feigenson. 1981. Fluorescence quenching in model membranes. An analysis of the local phospholipid environments of diphenylhexatriene and gramicidin A. *Biochim. Biophys. Acta.* 649: 89–97.

McConnell, H. M., and M. Vrljic. 2003. Liquid-liquid immiscibility in membranes. *Annu. Rev. Biophys. Biomol. Struct.* 32:469–492.

Mescher, M. F., and J. R. Apgar. 1985. The plasma membrane ''skeleton'' of tumor and lymphoid cells: a role in cell lysis? *Adv. Exp. Med. Biol.* 184:387–400.

Pralle, A., P. Keller, E.-L. Florin, K. Simons, and J. K. H. Hörber. 2000. Sphingolipid-cholesterol rafts diffuse as small entities in the plasma membrane of mammalian cells. *J. Cell Biol.* 148:997–1007.

Recktenwald, D. J., and H. M. McConnell. 1981. Phase equilibria in binary mixtures of phosphatidylcholines and cholesterol. *Biochemistry.* 20:4505–4510.

Ribeiro, A. A., and E. A. Dennis. 1973. Effect of thermotropic phase transitions of dipalmitoylphosphatidylcholine on the formation of mixed micelles with Triton X-100. *Biochim. Biophys. Acta.* 332:26–35.

Rinia, H. A., M. M. E. Snel, J. P. J. M. van der Earden, and B. de Kruiff. 2001. Visualizing detergent resistant domains in model membranes with atomic force microscopy. *FEBS Lett.* 501:92–96.

Samsonov, A. V., I. Mihalyov, and F. S. Cohen. 2001. Characterization of cholesterol-sphingomyelin domains and their dynamics in bilayer membranes. *Biophys. J.* 81:1486–1500.

Sankaram, M. B., and T. E. Thompson. 1990. Interaction of cholesterol with various glycerophospholipids and sphingomyelin. *Biochemistry.* 29:10670–10675.

Saslowsky, D. E., J. Lawrence, X. Ren, D. A. Brown, R. M. Henderson, and M. J. Edwardson. 2002. Placental alkaline phosphatase is efficiently targeted to rafts in supported lipid bilayers. *J. Biol. Chem.* 277:26966–26970.

Schroeder, R., E. London, and D. Brown. 1994. Interactions between saturated acyl chains confer detergent resistance on lipids and glycophosphatidylinositol (GPI)-anchored proteins: GPI-anchored proteins in liposomes and cells show similar behavior. *Proc. Natl. Acad. Sci. USA.* 91:12130–12134.

Schütz, G. J., G. Kada, V. P. Pastushenko, and H. Schindler. 2000. Properties of lipid microdomains in a muscle cell membrane visualized by single molecule microscopy. *EMBO J.* 19:892–901.

Silvius, J. R., D. del Giudice, and M. Lafleur. 1996. Cholesterol at different bilayer concentrations can promote or antagonize lateral segregation of phospholipids of differing acyl chain length. *Biochemistry.* 35:15198–15208.

Simons, K., and G. van Meer. 1988. Lipid sorting in epithelial cells. *Biochemistry*. 27:6197–6202.

Simons, K., and E. Ikonen. 1997. Functional rafts in cell membranes. *Nature*. 387:569–572.

Simons, K., and E. Ikonen. 2000. How cells handle cholesterol. *Science*. 290:1721–1726.

Smith, B. A., and H. M. McConnell. 1978. Determination of molecular motion in membranes using periodic pattern photobleaching. *Proc. Natl. Acad. Sci. USA*. 75:2759–2763.

Stryer, L. 1978. Fluorescence energy transfer as a spectroscopic ruler. *Annu. Rev. Biochem*. 47:819–846.

Tamm, L. K. 1988. Lateral diffusion and fluorescence microscope studies on a monoclonal antibody specifically bound to supported phospholipids bilayers. *Biochemistry*. 27:1450–1457.

Tamm, L. K., and H. M. McConnell. 1985. Supported phospholipid bilayers. *Biophys. J*. 47:105–113.

Tamm, L. K., and S. A. Tatulian. 1997. Infrared spectroscopy of proteins and peptides in lipid bilayers. *Quart. Rev. Biophys*. 30:365–429.

Thompson, T. E., M. B. Sankaram, R. L. Biltonen, D. Marsh, and W. L. C. Vaz. 1995. Effects of domain structure on in-plane reactions and interactions. *Mol. Membr. Biol*. 12:157–162.

van Meer, G., C. G. Gahmberg, and J. A. F. Op Den Kamp. 1981. Phospholipid distribution in human En(a-) red cell membranes which lack the major sialoglycoprotein, glycophorin A. *FEBS Lett*. 135: 53–55.

van Meer, G. 2002. The different hues of lipid rafts. *Science*. 296:855–857.

Veatch, S. L., and S. L. Keller. 2002. Organization of lipid membranes containing cholesterol. *Phys. Rev. Lett*. 89:2681011–2681014.

Wagner, M. L., and L. K. Tamm. 2000. Tethered polymer supported planar lipid bilayers for reconstitution of integral membrane proteins: silane-polyethyleneglycol-lipid as a cushion and covalent linker. *Biophys. J*. 79:1400–1414.

Wang, T., R. Leventis, and J. R. Silvius. 2000. Fluorescence-based evaluation of the partitioning of lipids and lipidated peptides into liquid-ordered lipid microdomains: a model for molecular partitioning in ''lipid rafts.'' *Biophys. J*. 79:919–933.

Wang, T., and J. R. Silvius. 2003. Sphingolipid partitioning into ordered domains in cholesterol-free and cholesterol-containing lipid bilayers. *Biophys. J*. 84:367–378.

Weast, R. C., editor. 1983. CRC Handbook of Chemistry and Physics, 64th Ed. CRC Press, Boca Raton, FL.

Wolber, P. K., and B. S. Hudson. 1979. An analytic solution to the Förster energy transfer problem in two dimensions. *Biophys. J*. 28:197–210.

Xu, X., and E. London. 2000. The effect of sterol structure on membrane lipid domains reveals how cholesterol can induce lipid domain formation. *Biochemistry*. 39:843–849.

Yuan, C., J. Furlong, P. Burgos, and L. J. Johnson. 2002. The size of lipid rafts: an atomic force microscopy study of ganglioside GM1 domains in sphingomyelin/DOPC/cholesterol membranes. *Biophys. J*. 82:2526–2535.